

# ME 502 Project Report

## Project #4 – Cooling Coil

### Jiong Chen

#### 1. Abstract

In this project, the heat transfer and hydrodynamics of a cooling coil is analyzed by applying finite volume concept. The cooling coil is a flat-tube-and-fin heat exchanger with only one slab. The profile of important parameters such as temperature, pressure and HTC along the tube of the heat exchanger is studied. A simplified condensation model is applied, and the results shows that increasing relative humidity can increase HTC of refrigerant and for higher air volumetric flow rate, the HTC of refrigerant is increased.

#### 2. Introduction

A cooling coil, also known as an evaporator coil, is a key component of an air conditioning system. It is responsible for removing heat and moisture from the air that is circulated through the system. Cooling coils are typically made of copper or aluminum tubes that are surrounded by a series of thin metal fins, which increase the surface area and improve heat transfer. The coils contain a refrigerant, which is a chemical that absorbs heat from the air as it passes over the coils, causing the refrigerant to evaporate. This process cools the air and removes moisture, which is then drained away. Cooling coils are crucial to the proper functioning of an air conditioning system, and proper maintenance and cleaning is essential to ensure their longevity and efficiency.

In this work, python code with CoolProp package is used to simulate a cooling coil given the geometry and operating conditions of the cooling coil. A simplified condensation model is applied in the program when the surface temperature is lower than the dew point temperature. First, with given operating condition, the overall performance of the cooling coil is predicted. Then different relative humidity and volumetric flow rate of air are applied to investigate the impact to the performance of the cooling coil.

#### 3. Methods and Assumptions

##### 3.1 Geometries and Operation Conditions

The operating fluid is the water-ethylene glycol (EG) solution with a mass fraction of 50% for ethylene. The humid air stream and the coolant stream are in a cross-flow arrangement. The detailed geometry and operation conditions of the cooling coil is listed in Table 1-3.

Table 1. Dimensions of the tubes of the cooling coil

Tube Geometry	Size
N_slab: number of slabs (rows), [-]	1
N_pass: number of passes in one slab, [-]	1
L_tube_pass: tube length in one pass, [mm]	300
N_tube_pass: number of tubes in one pass, [-]	23
t_wall*: wall thickness, [mm]	0.35
t_tube: tube thickness, [mm]	3
D_tube: tube depth, tube major, [mm]	35
n_port: number of ports in one tube, [-]	11
Ra_tube: roughness of tube inner surface, [m]	$10^{-6}$

\*  $t_{\text{wall}}$ : assume all the outer walls and inner walls have the same thickness.

Table 2. Dimensions of the fins of the cooling coil

Fin Geometry	Size
$\theta_{\text{louver}}$ : louver angle, [deg]	15
$P_{\text{louver}}$ : louver pitch, [mm]	1.3
$L_{\text{louver}}$ : louver length, [mm]	7.2
$N_{\text{louverbank}}$ : number of louver sets per fin [-]	2
$h_{\text{fin}}$ : fin height, [mm]	8
$t_{\text{fin}}$ : fin thickness, [mm]	0.1
$P_{\text{fin}}$ : fin pitch, [mm]	1.8 (14 FPI*)
$D_{\text{fin}}$ : fin depth, [mm]	35

\* FPI: fin per inch

Table 3. Operating Conditions

Parameter	Value
$T_{\text{ccegi}}$ : water-EG inlet temperature, [°C]	0
$p_{\text{ccegi}}$ : water-EG inlet pressure, [kPaA]	150
$\text{vol\_dot\_ccegi}$ : water-EG inlet volumetric flow rate, [L/min]	30
$T_{\text{ccai}}$ : air inlet temperature, [°C]	27
$p_{\text{ccai}}$ : air inlet pressure, [kPaA]	99.5
$\phi_{\text{ccai}}$ : air inlet relative humidity, [-]	0.5
$\text{vol\_dot\_ccai}$ : air inlet volumetric flow rate, [CFM]	500

The schematic of the cooling coil is shown in Figure 1. Assumptions were made: uniform distribution of refrigerant and air flow. Thus, only one tube calculation is needed. The tube will be divided into “n” small segments. Calculation will start from the 1<sup>st</sup> element. The output of the current element will be the input condition of the next element.

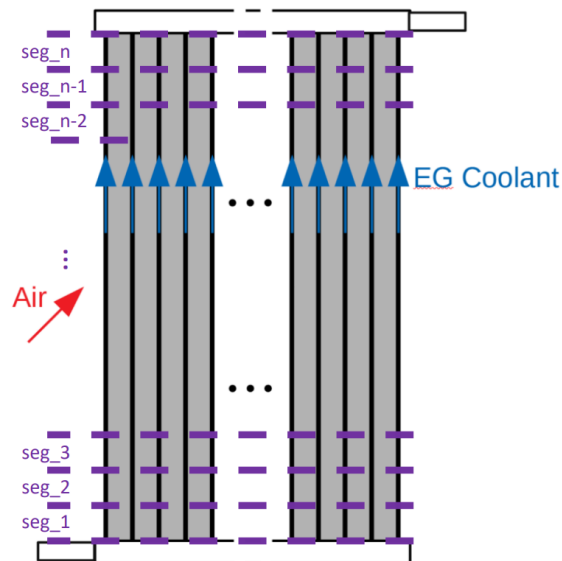


Figure 1. Schematic of cooling coil

### 3.2 Simplified Condensation Model

In the program, air is humid air, so condensation could happen. A simplified condensation model is applied. The schematic of the simplified condensation model is shown in Figure 2. The key assumptions of this model are: the temperature of water-EG-side surface of the wall  $T_{s,eg}$  is uniform; the convection heat transfer coefficient  $HTC_{eg}$  is constant. The air side heat transfer rate is composed of latent heat transfer rate and sensible heat transfer rate.

The sensible heat transfer rate can be calculated by:

$$T_{a,o} = T_{s,a} + (T_{a,i} - T_{s,a}) \exp\left(-\frac{HTC_a A_{s,a}}{\dot{m}_a c_{p,a}}\right)$$

$$Q_{a,sen} = \dot{m}_a c_{p,a} (T_{a,i} - T_{a,o})$$

The latent heat transfer rate can be obtained by analogy of sensible heat transfer rate:

$$MTC_a = \frac{HTC_a}{\rho_a c_{p,a} Le_a^{1-n}}, Le_a = \frac{\alpha_a}{D_{AB,a}}, D_{AB,a} = 0.26 \times 10^{-4} m^2/s, n = \frac{1}{3}$$

$$\rho_{A,o} = \rho_{A,s} + (\rho_{A,i} - \rho_{A,s}) \exp\left(-\frac{MTC_a A_{s,a}}{\dot{V}_a}\right)$$

$$\omega_{a,o} = \frac{\rho_{A,o}}{\rho_{da,o}} = \frac{\rho_{A,o}}{\rho_{da,i}} = \rho_{A,o} v_{da,i}$$

$$\dot{m}_{condensate} = \dot{m}_{da} (\omega_{a,i} - \omega_{a,o})$$

$$Q_{a,lat} = \dot{m}_{condensate} h_{fg}$$

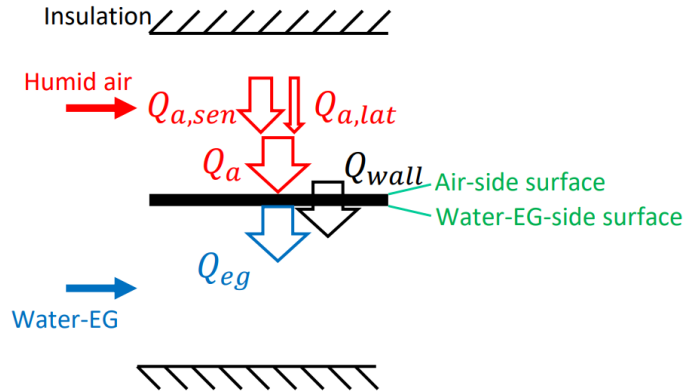


Figure 2. Schematic of simplified condensation model

From the schematic of simplified condensation model, the fin geometry is simplified to a plane-tube wall. However, when calculating the air-side surface area, the overall surface efficiency can be applied for the sensible heat transfer calculation; and for latent heat transfer calculation, the overall surface efficiency for mass transfer can be approximated as  $\eta_{o,m} = \eta_o^{0.5}$ .

EG side heat transfer rate can be calculated:

$$T_{eg,o} = T_{s,a} - (T_{s,a} - T_{eg,i}) \exp \left( - \frac{1}{\dot{m}_{eg} c_{p,eg} [R_{wall} + 1/(HTC_{eg} A_{s,eg})]} \right)$$

$$Q_{eg} = \dot{m}_{eg} c_{p,eg} (T_{eg,o} - T_{eg,i})$$

In the above equations, the air side surface temperature was first assumed by 1°C lower than the dew point and iterated to the condition when  $Q_{eg} = Q_{a,sen} + Q_{a,lat}$ .

### 3.3 Heat transfer rate for EG

When the Reynolds number is above 2300, Gnielinski's correlation [1] is used for determining Nusselt number:

$$Nu = \frac{f/8(Re - 1000)Pr}{1 + 12.7(f/8)^{1/2}(Pr^{2/3} - 1)}$$

$$f = [0.79 \ln(Re) - 1.64]^{-2}$$

When the Reynolds number is lower than 2300, Nusselt number is obtained by interpolation of data in Figure 3.



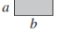
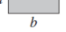
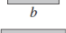
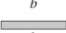
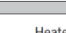


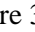
Cross Section	$\frac{b}{a}$	$Nu_D = \frac{HTC \cdot D_h}{k}$	
		(Uniform $q_s'$ )	(Uniform $T_s$ )
	—	4.36	3.66
	1.0	3.61	2.98
	1.43	3.73	3.08
	2.0	4.12	3.39
	3.0	4.79	3.96
	4.0	5.33	4.44
	8.0	6.49	5.60
	$\infty$	8.23	7.54
	$\infty$	5.39	4.86
	—	3.11	2.49

Figure 3. Laminar Flow Nusselt Number Table

### 3.4 Heat transfer rate for air

The air side heat transfer can be obtained with the correlation provided by Chang and Wang [2]:

$$htc_{air} = \rho_{air} \times Vel_{air} \times Cp_{air} \times St$$

$$St = j \times Pr_{air}^{-2/3}$$

$$j = Re_{Lp}^{-0.49} \left( \frac{\theta_{louver}}{90} \right)^{0.27} \left( \frac{P_{fin}}{P_{louver}} \right)^{-0.14} \left( \frac{h_{fin}}{P_{louver}} \right)^{-0.29} \left( \frac{D_{tube}}{P_{louver}} \right)^{-0.23}$$

$$\left( \frac{L_{louver}}{P_{louver}} \right)^{0.68} \left( \frac{P_{tube}}{P_{louver}} \right)^{-0.28} \left( \frac{t_{fin}}{P_{louver}} \right)^{-0.05}$$

### 3.5 Air side Hydraulic Performance

Air side pressure drop is calculated by the equation set provided by Chang and Wang [2]:

$$f = f_1 f_2 f_3$$

When  $Re_{Lp} < 150$ :

$$\begin{aligned} f_1 &= 14.39 Re_{Lp}^{-0.805 \frac{P_{fin}}{D_{fin}}} \ln^{3.04} \left( 1 + \frac{P_{fin}}{P_{louver}} \right) \\ f_2 &= \ln^{-1.435} \left( \left( \frac{t_{fin}}{P_{fin}} \right)^{0.48} + 0.9 \right) \left( \frac{D_{h,port}}{P_{louver}} \right)^{-3.01} \ln^{-3.01} (0.5 Re_{Lp}) \\ f_3 &= \left( \frac{P_{fin}}{L_{louver}} \right)^{-0.308} \left( \frac{D_{fin}}{L_{louver}} \right)^{-0.308} \exp(-0.1167 \frac{P_{tube}}{h_{fin}}) \theta_{louver}^{0.35} \end{aligned}$$

When  $150 < Re_{Lp} < 5000$ :

$$\begin{aligned} f_1 &= 4.97 Re_{Lp}^{0.6049 - 1.064/\theta^{0.2}} (\ln((t_{fin}/P_{fin})^{0.5} + 0.9))^{-0.527} \\ f_2 &= ((D_{h,port}/P_{louver}) \ln(0.3 Re_{Lp}))^{-2.966} (P_{fin}/L_{louver})^{-0.7931(P_{tube}/h_{fin})} \\ f_3 &= (P_{tube}/t_{tube})^{-0.0446} (\ln(1.2 + (P_{louver}/P_{fin})^{1.4}))^{-3.553} \theta_{louver}^{-0.477} \end{aligned}$$

The frictional factor  $f$  can also be expressed as:

$$f = \frac{A_c \rho_m}{A \rho_1} \left[ \frac{2 \rho_1 D P_{air}}{G_c^2} - (K_c + 1 - \sigma^2) - 2 \left( \frac{\rho_1}{\rho_2} - 1 \right) + (1 - \sigma^2 - K_e) \frac{\rho_1}{\rho_2} \right]$$

### 3.6 EG side Hydraulic Performance

The pressure drop of EG is calculated by correlation provided by Churchill [3]:

$$\begin{aligned} DP_{ref} &= DP_{ref,static} = \frac{\partial p}{\partial z_f} \frac{L_{elem}}{D_{h,port}} \frac{G_{ref}^2}{2 \rho_{ref}} \\ \frac{\partial p}{\partial z_f} &= 8 \left( \left( \frac{8}{Re_D} \right)^{12} + \left( \frac{1}{A+B} \right)^{1.5} \right)^{\frac{1}{12}} \\ A &= (-2.456 \ln^{0.9} \left( \frac{7}{Re_D} \right) + 0.27 \frac{Ra_{tube}}{D_{h,port}})^{16} \\ B &= \left( \frac{37530}{Re_D} \right)^{16} \end{aligned}$$

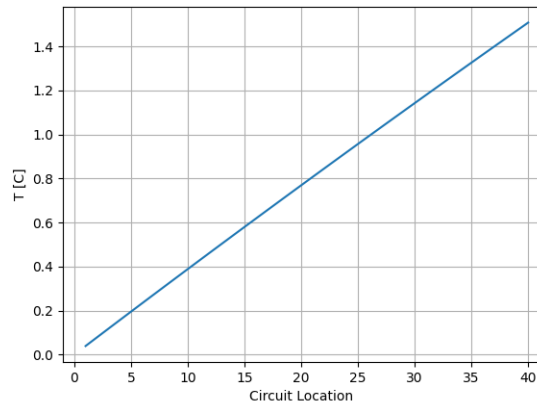
## 4. Results and Discussion

### 4.1 Overall Performance of Cooling Coil

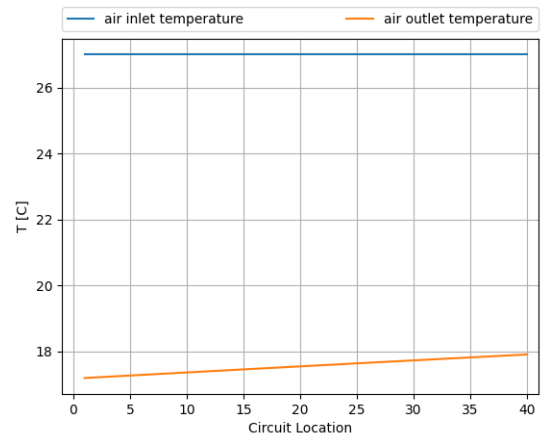
Figure 4 contains the plots of detailed overall performance of the cooling coil. The total performance of the cooling coil is presented in Table 4.

T_ccego	T_ccao	T_dp_ccao	P_ccego	Q_tot	Q_sen_tot	Q_lat_tot
1.51°C	17.56°C	12.82°C	146.41kPa	2.60kW	1.29kW	1.30kW

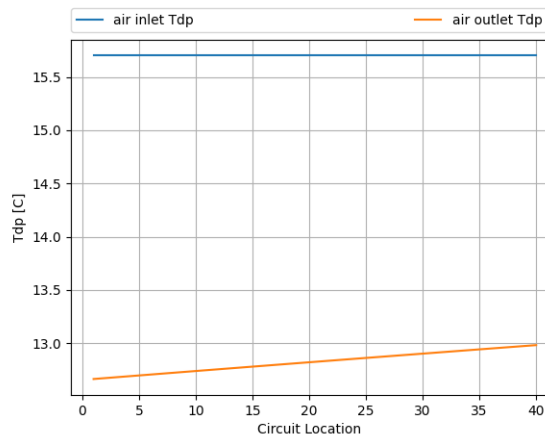
(a)



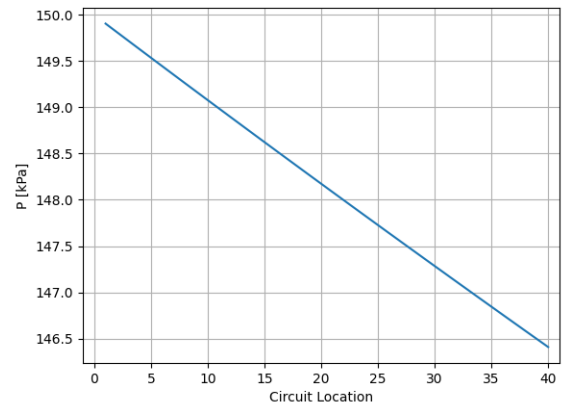
(b)



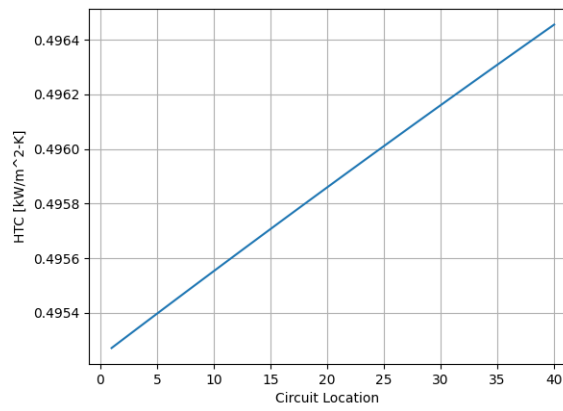
(c)



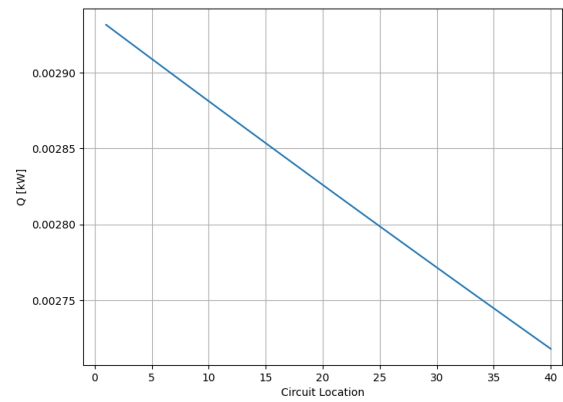
(d)



(e)



(f)



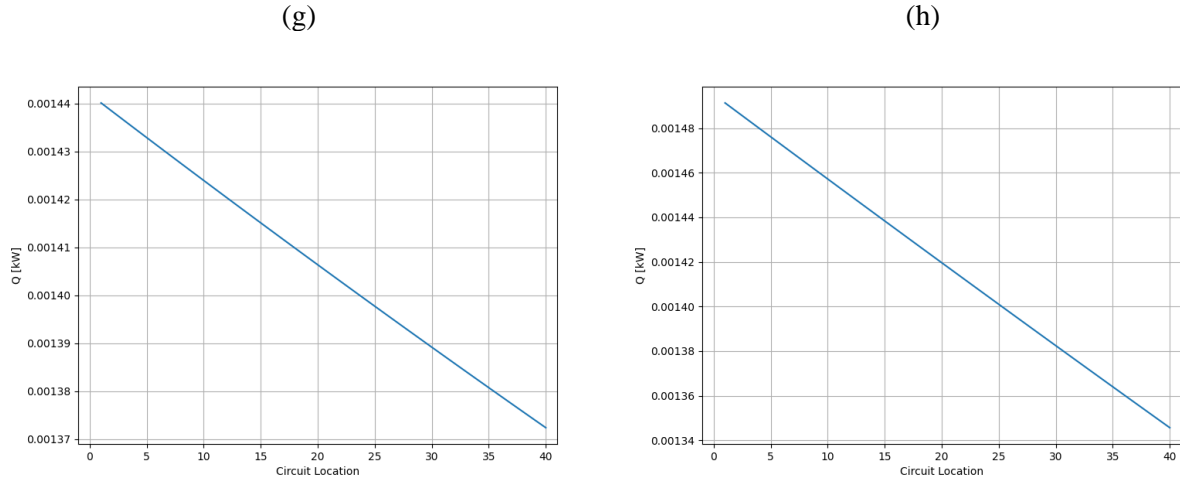
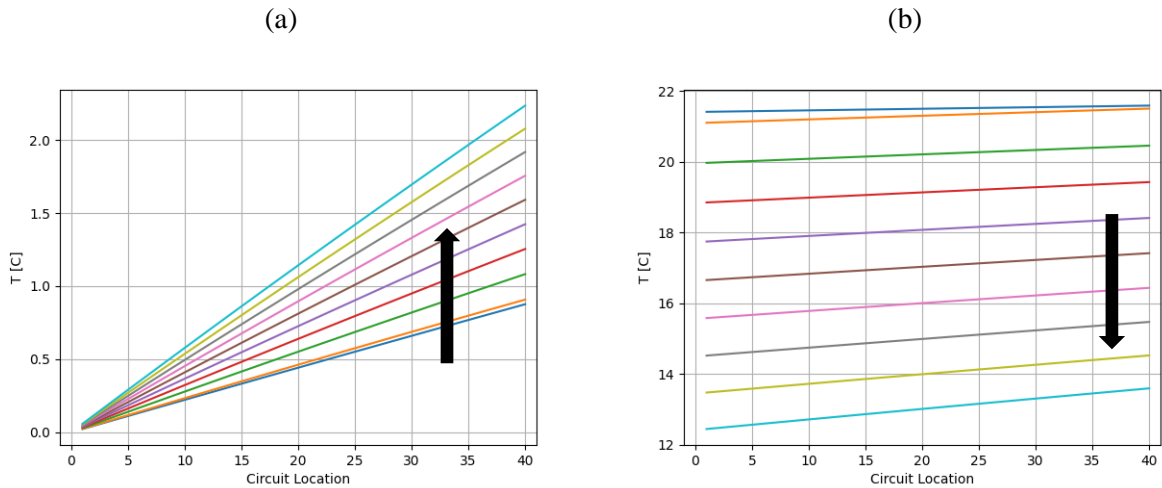


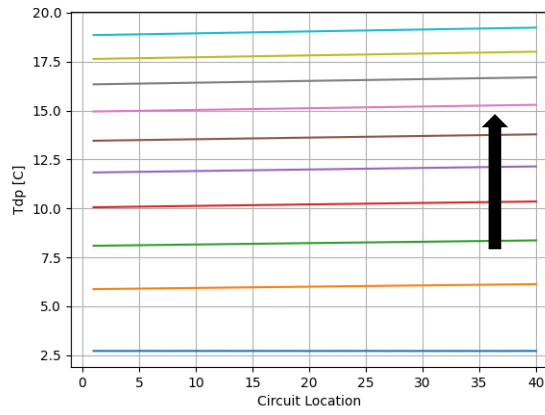
Figure 4. Overall Performance of cooling coil. (a) EG temperature distribution; (b) Air inlet and outlet dry bulb temperature; (c) air inlet and outlet dew point temperature; (d) EG pressure distribution; (e) EG heat transfer coefficient distribution; (f) Total heat transfer rate in each segment; (g) sensible heat transfer rate in each segment; (h) latent heat transfer rate in each segment.

Notice that as the EG temperature increases, the heat transfer coefficient of EG increases, but because the temperature difference between EG and air flow decreases, the heat transfer rate decreases. While EG temperature increases, air side surface temperature increases, and the latent heat transfer rate decreases. The trend of heat transfer rate, temperature and pressure are almost linear through the tube.

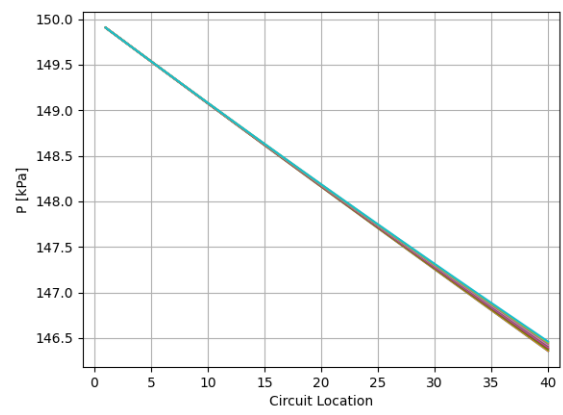
#### 4.2 Impact of Relative Humidity



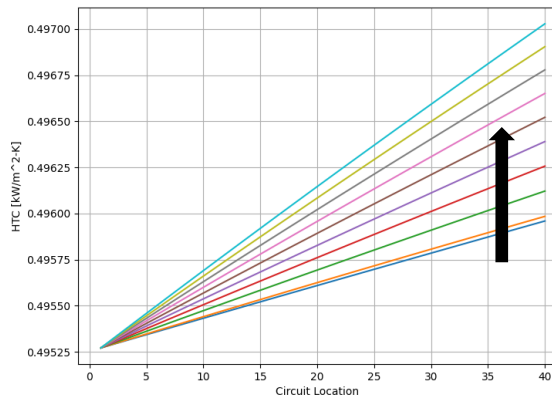
(c)



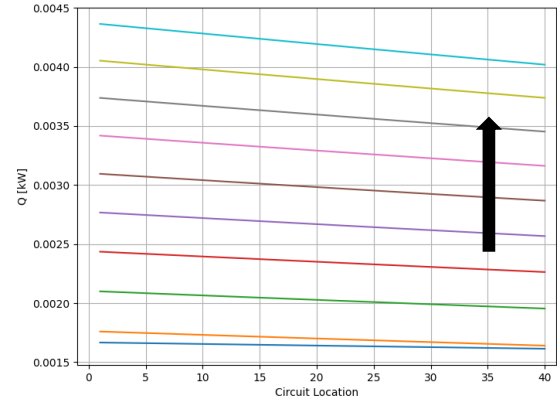
(d)



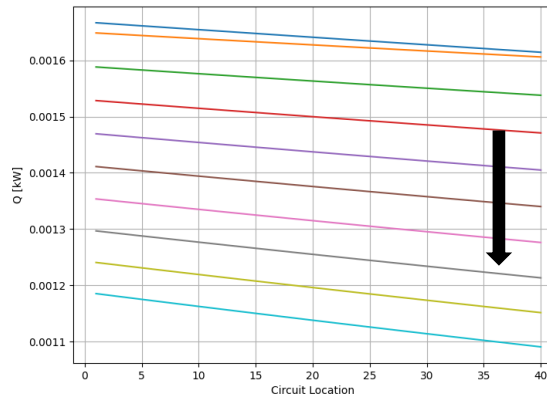
(e)



(f)



(g)



(h)

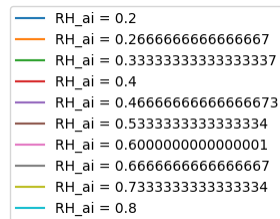
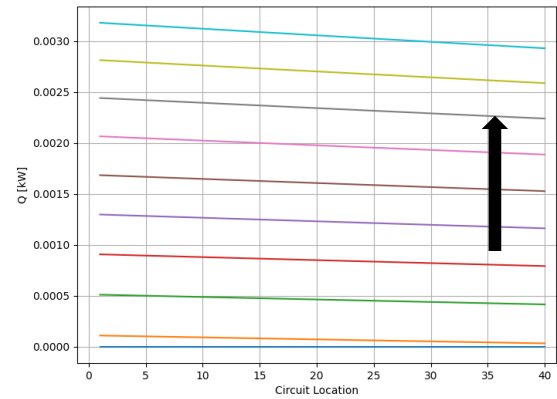
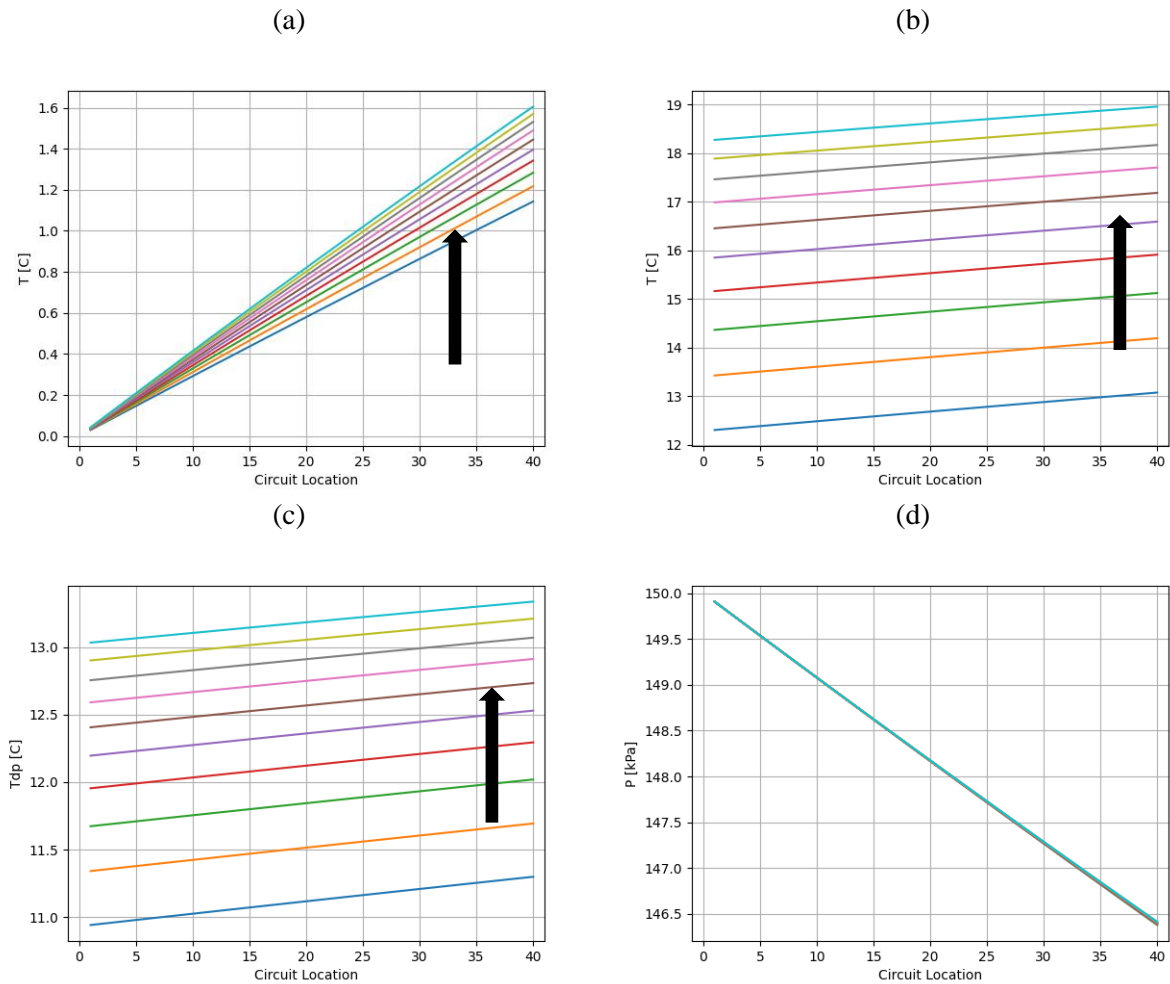




Figure 5. Impact of relative humidity on the performance of cooling coil. (a) EG Temperature; (b) Air outlet temperature; (c) air outlet dew point temperature; (d) EG pressure; (e) EG heat transfer coefficient; (f) segment heat transfer rate; (g) segment sensible heat transfer rate; (h) segment latent heat transfer rate.

The arrow direction indicates the increasing relative humidity. As the relative humidity rises, the outlet temperature of the EG increases from 0.9°C to 2.4°C, while the air outlet temperature decreases from 21.5°C to 11°C. Furthermore, an increase in the inlet relative humidity results in a rise in the outlet air dew point temperature from 2.5°C to 19°C. This outcome is reasonable because higher relative humidity entails more water vapor being fed into the cooling coil, resulting in more water vapor remaining at the cooling coil outlet. The pressure drop of EG is unaffected by the change in relative humidity, as shown in Figure 5(d). The heat transfer coefficient of EG increases as the relative humidity increases because EG temperature rises more quickly. Consequently, more condensation occurs at higher relative humidity, resulting in a significant increase in total heat transfer rate from 0.0015W per segment to 0.0043W per segment. Sensible and latent heat transfer rates are both affected by the relative humidity, with an increase in the weight of latent heat transfer rate and a decrease in the weight of sensible heat transfer rate as relative humidity increases.

#### 4.3 Impact of Volumetric Flow Rate



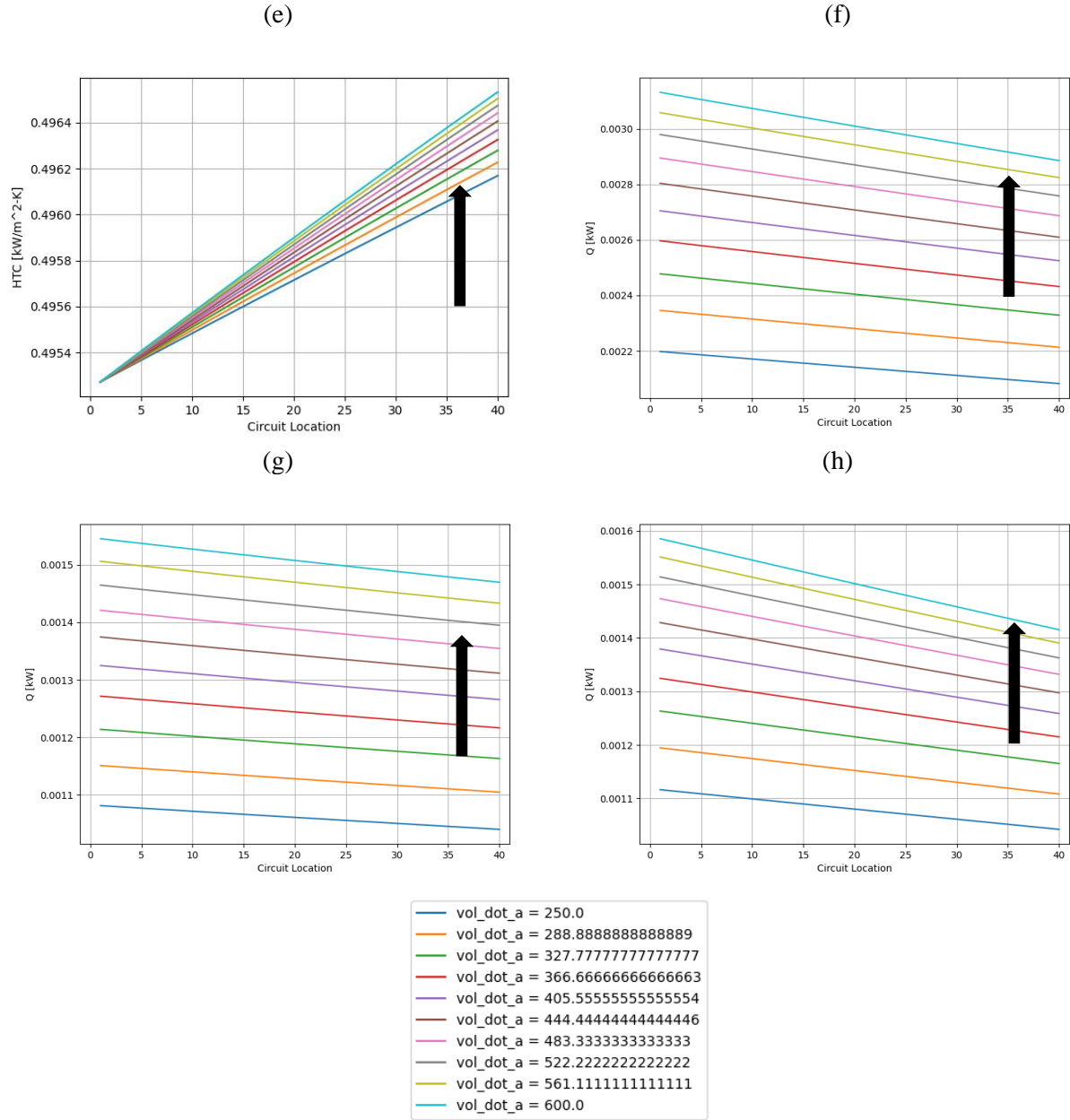


Figure 6. Impact of volumetric flow rate on the performance of cooling coil. (a) EG Temperature; (b) Air outlet temperature; (c) air outlet dew point temperature; (d) EG pressure; (e) EG heat transfer coefficient; (f) segment heat transfer rate; (g) segment sensible heat transfer rate; (h) segment latent heat transfer rate. Unit for volumetric flow rate is CFM.

The arrow direction in the figure denotes an increase in air volumetric flow rate. An increase in air volumetric flow rate results in an increase in the rate at which the EG temperature rises, with outlet EG temperature increasing from 1.15°C to 1.6°C. As more air flows through the cooling coil during the same amount of time, the air outlet temperature also increases from 13°C to 19°C. Additionally, the air outlet dew point temperature increases from 11.3°C to 13.4°C. The air volumetric flow rate has a negligible effect on EG pressure drop. The heat transfer coefficient (HTC) of EG increases with a higher volumetric flow rate. The total heat transfer rate increases from 0.0021W per segment to 0.0030W per segment.

Unlike relative humidity, both sensible heat transfer rate and latent heat transfer rate increase as the volumetric flow rate increases.

## **5. Conclusions**

The heat transfer and hydraulic performance of a cooling coil was simulated with python and package CoolProp. The simplified condensation model is applied for the condition that surface temperature is lower than the dew point temperature. The overall performance and parameters of interest were shown. Impacts of relative humidity and air volumetric flow rate were investigated and compared. When increasing the relative humidity, the sensible heat transfer rate decreased while the latent heat transfer rate increased; however, when increasing the air volumetric flow rate, both sensible heat transfer rate and latent heat transfer rate increased.

## **6. References**

- [1] Gnielinski, Volker. "New equations for heat and mass transfer in the turbulent flow in pipes and channels." NASA STI/recon technical report A 41.1 (1975): 8-16.
- [2] Chang, Y-JY-J., et al. "A generalized friction correlation for louver fin geometry." International journal of heat and mass transfer 43.12 (2000): 2237-2243.
- [3] Churchill, Stuart W. "Friction-factor equation spans all fluid-flow regimes." (1977).